Kinoform diffractive lenses for efficient nano-focusing of hard X-rays

Petri Karvinen,[1,2,*] Daniel Grolimund,[1] Markus Willimann,[1,3] Beat Meyer,[1] Mario Birri,[1] Camelia Borca,[1] Jens Patommel,[4] Gerd Wellenreuther,[5,6] Gerald Falkenberg,[5] Manuel Guizar-Sicairos,[1] Andreas Menzel,[1] and Christian David[1]

[1]*Paul Scherrer Institut, CH 5232 Villigen-PSI, Switzerland*
[2]*Currently with Institute of Photonics, University of Eastern Finland, FI-80100 Joensuu, Finland*
[3]*Currently with DECTRIS AG, Neuenhoferstrasse 107, CH 5400 Baden, Switzerland*
[4]*Institute of Structural Physics, Technische Universität Dresden, D-01062 Dresden, Germany*
[5]*HASYLAB at DESY, Notkestr. 85, D-22607 Hamburg, Germany*
[6]*Currently with European XFEL GmbH, Notkestr. 85, D-22607 Hamburg, Germany*
[*]*petri.karvinen@uef.fi*

Abstract: A nano-focusing module based on two linear Fresnel zone plates is presented. The zone plates are designed to generate a kinoform phase profile in tilted geometry, thus overcoming the efficiency limitations of binary diffractive structures. Adjustment of the tilt angle enables tuning of the setup for optimal efficiency over a wide range of photon energies, ranging from 5 to 20 keV. Diffraction efficiency of more than 50% was measured for the full module at 8 keV photon energy. A diffraction limited spot size of 100 nm was verified by ptychographic reconstruction for a lens module with a large entrance aperture of 440 μm × 400 μm.

OCIS codes: (050.1965) Diffractive lenses; (340.6720) Synchrotron radiation; (340.7460) X-ray microscopy.

References and links

1. P. Kirkpatrick and A. V. Baez, "Formation of optical images by x-rays," J. Opt. Soc. Am. **38**(9), 766–774 (1948).
2. A. Snigirev, V. Kohn, I. Snigireva, and B. Lengeler, "A compound refractive lens for focusing high-energy x-rays," Nature **384**(6604), 49–51 (1996).
3. B. Lengeler, C. G. Schroer, M. Richwin, J. Tümmler, M. Drakopoulos, A. Snigirev, and I. Snigireva, "A microscope for hard x rays based on parabolic compound refractive lenses," Appl. Phys. Lett. **74**(26), 3924 (1999).
4. A. Schropp, R. Hoppe, V. Meier, J. Patommel, F. Seiboth, H. J. Lee, B. Nagler, E. C. Galtier, B. Arnold, U. Zastrau, J. B. Hastings, D. Nilsson, F. Uhlén, U. Vogt, H. M. Hertz, and C. G. Schroer, "Full spatial characterization of a nanofocused x-ray free-electron laser beam by ptychographic imaging," Sci Rep **3**, 1633 (2013).
5. V. V. Aristov, M. Grigoriev, S. Kuznetsov, L. Shabelnikov, V. Yunkin, T. Weitkamp, C. Rau, I. Snigireva, A. Snigirev, M. Hoffmann, and E. Voges, "X-ray refractive planar lenses with minimized absorption," Appl. Phys. Lett. **77**(24), 4058 (2000).
6. L. Alianelli, K. J. S. Sawhney, M. K. Tiwari, I. P. Dolbnya, R. Stevens, D. W. K. Jenkins, I. M. Loader, M. C. Wilson, and A. Malik, "Characterization of germanium linear kinoform lenses at Diamond Light Source," J. Synchrotron Radiat. **16**(3), 325–329 (2009).
7. B. Nöhammer, J. Hoszowska, A. K. Freund, and C. David, "Diamond planar refractive lenses for third- and fourth-generation x-ray sources," J. Synchrotron Radiat. **10**(2), 168–171 (2003).
8. C. G. Schroer, O. Kurapova, J. Patommel, P. Boye, J. Feldkamp, B. Lengeler, M. Burghammer, C. Riekel, L. Vincze, A. van der Hart, and M. Küchler, "Hard x-ray nanoprobe based on refractive x-ray lenses," Appl. Phys. Lett. **87**(12), 124103 (2005).
9. G. Schmahl and D. Rudolph, "High power zone plates as image forming systems for soft x-rays," Optik (Stuttg.) **29**, 577 (1969).
10. J. Vila-Comamala, K. Jefimovs, J. Raabe, T. Pilvi, R. H. Fink, M. Senoner, A. Maassdorf, M. Ritala, and C. David, "Advanced thin film technology for ultrahigh resolution x-ray microscopy," Ultramicroscopy **109**(11), 1360–1364 (2009).
11. J. Kirz, "Phase zone plates for x rays and the extreme UV," J. Opt. Soc. Am. **64**(3), 301–309 (1974).
12. J. A. Jordan, Jr., P. M. Hirsch, L. B. Lesem, and D. L. Van Rooy, "Kinoform lenses," Appl. Opt. **9**(8), 1883–1887 (1970).

#208741 - $15.00 USD Received 24 Mar 2014; revised 12 Jun 2014; accepted 15 Jun 2014; published 30 Jun 2014

13. K. Evans-Lutterodt, A. Stein, J. M. Ablett, N. Bozovic, A. Taylor, and D. M. Tennant, "Using compound kinoform hard-x-ray lenses to exceed the critical angle limit," Phys. Rev. Lett. **99**(13), 134801 (2007).
14. A. F. Isakovic, A. Stein, J. B. Warren, S. Narayanan, M. Sprung, A. R. Sandy, and K. Evans-Lutterodt, "Diamond kinoform hard X-ray refractive lenses: design, nanofabrication and testing," J. Synchrotron Radiat. **16**(1), 8–13 (2009).
15. E. Di Fabrizio, F. Romanato, M. Gentili, S. Cabrini, B. Kaulich, J. Susini, and R. Barrett, "High-efficiency multilevel zone plates for keV X-rays," Nature **401**(6756), 895–898 (1999).
16. I. Mohacsi, P. Karvinen, I. Vartiainen, V. A. Guzenko, A. Somogyi, C. Kewish, P. Mercere, and C. David, "High efficiency X-ray nanofocusing by multilevel zone plates," J. Synchrotron Radiat. (to be published).
17. B. Nöhammer, C. David, M. Burghammer, and C. Riekel, "Coherence-matched micro focusing of hard x-rays," Appl. Phys. Lett. **86**(16), 163804 (2005).
18. C. David, B. Nöhammer, and E. Ziegler, "A wavelength tunable diffractive transmission lens for hard x-rays," Appl. Phys. Lett. **79**(8), 1088–1090 (2001).
19. S. Gorelick, V. A. Guzenko, J. Vila-Comamala, and C. David, "Direct e-beam writing of dense and high aspect ratio nanostructures in thick layers of PMMA for electroplating," Nanotechnology **21**(29), 295303 (2010).
20. C. David, S. Gorelick, S. Rutishauser, J. Krzywinski, J. Vila-Comamala, V. A. Guzenko, O. Bunk, E. Färm, M. Ritala, M. Cammarata, D. M. Fritz, R. Barrett, L. Samoylova, J. Grünert, and H. Sinn, "Nanofocusing of hard X-ray free electron laser pulses using diamond based Fresnel zone plates," Sci Rep **1**, 57 (2011).
21. C. G. Schroer and B. Lengeler, "Focusing hard x rays to nanometer dimensions by adiabatically focusing lenses," Phys. Rev. Lett. **94**(5), 054802 (2005).
22. C. G. Schroer, P. Boye, J. M. Feldkamp, J. Patommel, D. Samberg, A. Schropp, A. Schwab, S. Stephan, G. Falkenberg, G. Wellenreuther, and N. Reimers, "Hard X-ray nanoprobe at beamline P06 at PETRA III," Nucl. Instrum. Meth. A **616**(2-3), 93–97 (2010).
23. M. Guizar-Sicairos and J. R. Fienup, "Measurement of coherent x-ray focused beams by phase retrieval with transverse translation diversity," Opt. Express **17**(4), 2670–2685 (2009).
24. M. Guizar-Sicairos, S. Narayanan, A. Stein, M. Metzler, A. R. Sandy, J. R. Fienup, and K. Evans-Lutterodt, "Measurement of hard x-ray lens wavefront aberrations using phase retrieval," Appl. Phys. Lett. **98**(11), 111108 (2011).
25. J. Vila-Comamala, A. Diaz, M. Guizar-Sicairos, A. Mantion, C. M. Kewish, A. Menzel, O. Bunk, and C. David, "Characterization of high-resolution diffractive X-ray optics by ptychographic coherent diffractive imaging," Opt. Express **19**(22), 21333–21344 (2011).

1. Introduction

Synchrotron-based chemical imaging techniques, like scanning x-ray fluorescence microscopy (SXFM), x-ray absorption spectromicroscopy (microXAS) and micro x-ray diffraction (microXRD), all require highly efficient focusing of hard x-rays. The desired spot size has moved from micro- to nano-regime, which places stringent requirements for the used focusing optics.

The most popular devices for focusing x-rays to small spot sizes are curved mirrors in the Kirkpatrick-Baez arrangement [1]. These systems have low losses, are achromatic, and micron spot sizes can be routinely achieved with various commercial systems. However, systems capable of 100 nm spot sizes or below are very complex and costly, as the manufacture and alignment of sufficiently perfect mirror surfaces requires tremendous effort. This is true especially when the mirrors are made long enough to accept relatively large beams of several hundred microns in cross section.

A simpler and more robust alternative are refractive lenses. Huge progress has been made since Snigirev *et al.* first demonstrated focusing of hard x-rays by a simple array of holes drilled into an aluminium block [2]. For better resolution, compound refractive lenses with parabolic shapes were developed [3] from aluminium, beryllium [4], or nickel. However, their transmission is poor at lower x-ray energies, i.e. in the range of a few keVs, and the resolution is limited by the residual shape errors. In order to exploit the flexibility and precision of nanolithography techniques to improve both transmission and resolution, planar refractive lenses were developed that consist of lens structures fabricated by etching into a planar substrate [5]. Devices from silicon, germanium [6], diamond [7], and other materials have been demonstrated. In these arrangements, the x-rays travel parallel to the substrate surface and are refracted from the side walls of the etched structures. Lenses made by this planar fabrication technique only focus in one dimension, and two such devices need to be arranged behind each other in perpendicular orientation for two-dimensional focusing - comparable to KB mirrors. The best resolution values for this type of setups have been reported by Schroer et al. [8]. Focusing down to a 47 nm x 55 nm spot size was obtained at 21 keV photon energy.

#208741 - $15.00 USD Received 24 Mar 2014; revised 12 Jun 2014; accepted 15 Jun 2014; published 30 Jun 2014

However, due to absorption losses, it is not possible to efficiently use such lenses with photon energies below 10 keV. Moreover, the aperture of the lenses is limited by the achievable etching depth, and apertures of only about 50 μm are possible when high resolution is required.

Diffractive lenses, i.e. Fresnel zone plates, have been used for several decades for high-resolution x-ray microscopy [9]. The resolution of these devices is essentially limited to the width of the smallest (outermost) zone structures. In scanning x-ray microscopy, very high resolution spot sizes on the order of 10 nm have been obtained in the soft x-ray range [10]. The main drawback of Fresnel zone plates is the limited diffraction efficiency, which is typically around 5-10%. This problem becomes even more severe with higher photon energies, as the required zone structures need to be much higher than their width. But even in the idealized case of zone plate structures having no absorption and sufficient height to introduce a π phase shift, the diffraction efficiency of a Fresnel zone plate with binary structures is limited to below 40.5% [11]. In order to bypass this limitation, kinoform x-ray lenses that have asymmetric zone profiles to introduce a continuous modulo 2π phase shift are required [12–14]. Approximations of such lenses have been realized for the x-ray range as multilevel zone plates [15,16]. These devices can indeed provide a better efficiency than binary structures. However, the required nanofabrication steps are extremely challenging, which has so far limited the resolution of multilevel zone plates to several hundred nanometers.

2. Concept of the kinoform diffractive lens

Our approach is to use two linear diffractive lenses in combination to achieve 2D focusing [17]. Normally the use of two diffractive lenses instead of one is not favored in x-ray optics due to low achievable efficiencies of each element. Thus this approach prioritizes the optimization of the lens efficiency.

For the best possible diffraction efficiency the aforementioned kinoform phase profiles have to be utilized. For hard x-ray regime the fabrication of diffractive structures high enough to provide optimal phase shift is a challenge. However, in case of one dimensionally focusing lenses one can increase the effective height of the structures by tilting [18]. Simultaneously the tilting can be used for the realization of a kinoform phase profile with binary structures like depicted in Fig. 1: instead of normal line structures the lens is patterned into stripes of triangles that are shaped to approximate the optimal kinoform phase profile within the accuracy of the fabrication processes. The incoming beam incident at a shallow angle passes through a large number of these lenslets, and thus the effective phase profile equals the sum of these profiles passed through multiplied by a constant that depends on the material properties and angle of incidence.

By changing the tilting of the lens the effective structure height can be tuned to give the optimal phase shift for different wavelengths. The optimal incident angle α, i.e. the angle between the lens surface and the incident beam, can be calculated from the geometry to be

$$\alpha = \arcsin\left(\frac{h\delta}{\lambda}\right), \tag{1}$$

where λ is the wavelength, h is the height of the fabricated lens structure and δ denotes the material dispersion, i.e. the difference of the real part of the refractive index of the material from unity. In this geometry the lens produces 2π phase shift for the x-rays traveling through the thickest parts of the lens. It is worth noting that by this definition the angle α = 0° the lens structure is completely parallel to the beam and increasing α always enlarges the aperture size; this is according the convention when using refractive kinoform lenses, but differs from the normal usage of linear diffractive lenses where one usually defines a tilt angle that is zero when the structure is perpendicular to the beam.

#208741 - $15.00 USD Received 24 Mar 2014; revised 12 Jun 2014; accepted 15 Jun 2014; published 30 Jun 2014

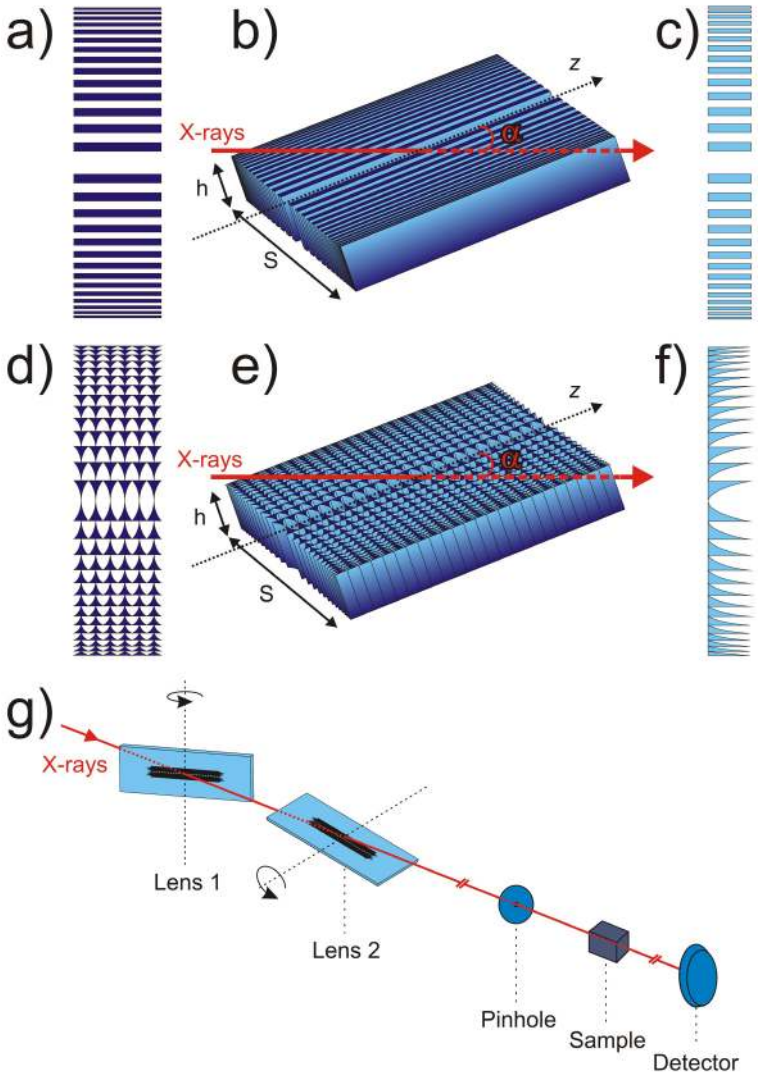

Fig. 1. Schematic comparison of the normal linear diffractive lens and one with kinoform wavefront producing structures. a and d: top views of the patterns, b and e: schematics of the usage in tilted geometry, c and f: resulting effective phase profile of the normal and kinoform lenses, respectively. The schematic view of the entire two lens setup is shown in g.

It is essential to note the following key features of these lenses:

(i) Achieving the ideal kinoform phase profile for high efficiency focusing does not require structures with continuous height profiles; it can be obtained with binary structures.

(ii) By adjusting the angle of incidence, the ideal phase profile can be obtained for different photon energies. The same set of lenses can therefore be used for efficient focusing over a wide energy range.

(iii) Any deviation of the diffractive structures from their ideal shape reduces the local diffraction efficiency of the device by either increasing absorption or diffracting part of the intensity to unwanted diffraction orders. However, unlike planar refractive lenses made by etching kinoform profiles into planar substrates this does not have

#208741 - $15.00 USD Received 24 Mar 2014; revised 12 Jun 2014; accepted 15 Jun 2014; published 30 Jun 2014

any impact on the achievable spot size. The spot size is only limited by the placement error of the zone structures which is negligible with the current electron beam lithography tools.

(iv) Unlike planar refractive x-ray lenses, the accepted beam size is not limited to the depth of the structures. In consequence, the depth can be chosen to be fairly shallow, allowing for diffractive structures with smaller lateral dimensions and therefore higher resolution.

3. Materials and methods

For use in different energy ranges and applications lenses were fabricated out of three different materials: gold (Au), nickel (Ni), and diamond (C). Au and Ni lenses were made by electroplating into a polymethyl methacrylate (PMMA) mold fabricated using electron beam lithography (EBL) [19]. The diamond lenses were made by reactive ion etching of a diamond membrane using a hydrogen silsesquioxane (HSQ) patterned by EBL as etching mask. The diamond membranes used were CVD grown polycrystalline membranes normally used as x-ray windows that are commercially available (Diamond Materials Gmbh). A detailed process description can be found in reference [20]. Scanning electron microscope images of the structures can be seen in Fig. 2. The height of the fabricated structures was typically 1 micron in gold and nickel and more than 2 microns in the case of diamond. As can be calculated using Eq. (1), a photon energy range of 5 – 20 keV results for incident angle α a range of 29° – 7° for gold, 16° – 4° for nickel and 14° – 3° for diamond lenses. The shallow illumination angles mean that for e.g. 400 micron aperture the patterned lens length needs to be from around one millimeter up to little over 5 millimeters. On the other hand the pitch of the outermost zones defines the diffraction limit of the spot size. In our case this means that the full width half maximum (FWHM) of the diffraction-limited spot is half of the pitch of the outermost triangular structures. For different lenses this pitch was varied between 400 nm and 200 nm, resulting in diffraction limits down to ≈100 nm.

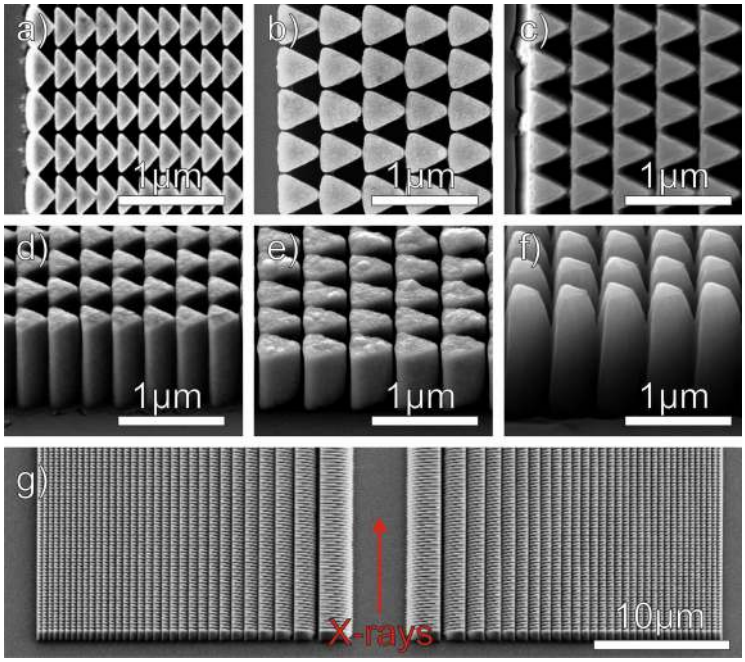

Fig. 2. SEM images of the fabricated structures. a-c: top view of nickel, gold and diamond structures, respectively. d-f: images in 50 degrees tilt angle of the same structures in the same order. g: overview of one end of a 50 µm wide untapered nickel lens in the same orientation as d-f.

#208741 - $15.00 USD Received 24 Mar 2014; revised 12 Jun 2014; accepted 15 Jun 2014; published 30 Jun 2014

When using large aperture linear lenses at shallow incident angles, the thin lens approximation becomes invalid. More specifically this happens when the tilted lens spans larger length in the beam propagation direction than the focal depth of the lens, meaning that the different parts of the lens produce the focus in different points along the optical axis. This can be corrected by making the lens adiabatically focusing, in analogy to adiabatic refractive lenses [21]. In our case this means that each part of the lens along the optical axis is designed according to the zone plate equation to produce focus in the same focal point. As a result, the lenses are tapered to narrow down towards the direction of the beam propagation. This can be achieved by designing the lens width S to be a function of the position along the lens length, z, according to following equation:

$$S(z) = S_0 + (h\delta - \lambda)\frac{2z}{d_r}. \quad (2)$$

Here S_0 denotes the designed lens width at the position $z = 0$, and d_r is the outermost pitch of the triangle structure (i.e. double the effective outermost zone width). This results in lenses with width S linearly narrowing towards the beam direction. The tapering naturally limits the use of a single lens design to only a certain bandwidth of photon energies, but this limitation is not too strict. As an example calculated for a 1 micron high nickel lens with 400 nm outermost pitch and 200 micron entrance aperture tapered for 11 keV photon energy according to Eq. (2), the upstream and the downstream parts of the lens produce foci within the focal depth of the lens for all the photon energies between 5 and 16 keV. Even in the extreme case of 200 nm outermost pitch and 400 micron entrance aperture a bandwidth of about 1.5 keV fulfills this relatively stringent criteria. This is more than enough for the majority of scanning spectroscopy applications, so there is no need to change lenses as long as they can be moved along the beam axis to compensate for the change in working distance.

Because of the use of separate elements for horizontal and vertical axis the transverse asymmetry of the source can be matched to obtain a symmetric spot with diffraction-limited focusing and largest possible acceptance of the incident beam [17]. In practice this means that even highly asymmetric apertures, e.g. 100 μm × 400 μm, can be used to compensate for the larger horizontal source size.

To position and align the lenses with required accuracy advanced mechanics have to be used. In our case the experimental setup at the microXAS and cSAXS beamlines at SLS was based on Smaract (www.smaract.de) stick-slip piezo positioners forming a complete mechanical module with all the necessary translations and rotations for both of the lenses, order-sorting aperture (OSA), and sample. Important for this application is the long movement range for the lenses along the beam axis enabling the use of wide variety of different focal lengths in an automated way. Thus this entire module was based on a 1 m long rail that allows working distances from 3 cm up to almost the full 1 m. This makes it possible to use similar lens designs over the wide photon energy bandwidth of 5 – 20 keV and even scanning the energy over a large range while automatically compensating for the change in the focal length and optimal incident angle. Typical working distances for e.g. the lenses providing 100 μm × 400 μm entrance aperture with 100 nm outermost pitch are 58 and 232 mm, respectively, at 7.2 keV photon energy. At the P06 beamline at PetraIII the lenses were mounted using the Attocube (www.attocube.com) nanopositioners normally used for the refractive nanofocusing lenses installed at the nanoprobe instrument on that beamline [22].

4. Results and discussion

Various lenses with different designs (outermost zone pitch, structure height, and with and without tapering) were tested and used at different photon energies at the microXAS and cSAXS beamlines (SLS) and at the beamline P06 (PetraIII). The diffraction efficiencies measured for the two-lens setup are shown with theoretical curves for perfect phase-wrapped parabolic lenses in Fig. 3 (left plot). The effect of the lens tilt is shown in the right plot where the measured efficiency at 8 keV for a system of two nickel lenses is depicted.

#208741 - $15.00 USD Received 24 Mar 2014; revised 12 Jun 2014; accepted 15 Jun 2014; published 30 Jun 2014

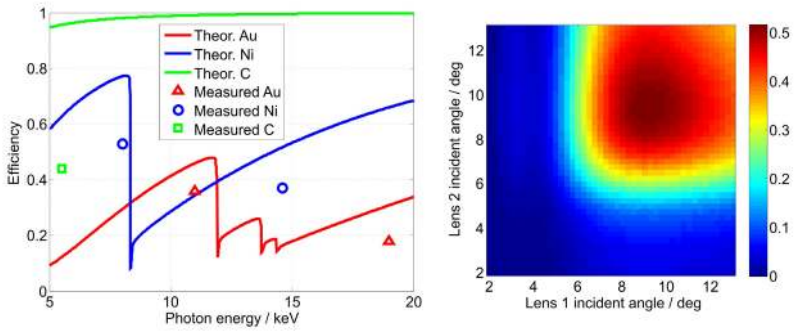

Fig. 3. Left: Theoretical and measured efficiencies of a 2D focusing system composed of two kinoform linear diffractive lenses as a function of the photon energy. Red denotes gold lenses, blue nickel and green diamond; solid lines are theoretical and traingles, circles and squares represent measured values. The theoretical curves are calculated for lenses with an ideal kinoform phase profile. Right: Measured total efficiency of a nickel lens system at 8 keV photon energy and a fixed aperture of 50 μm × 200 μm as a function of the incident angles on the individual lenses.

The best measured efficiency value was over 50% at 8 keV photon energy for a lens pair with 50 μm × 200 μm entrance aperture and 200 nm effective outermost zone width at the microXAS beamline. This indicates an efficiency of more than 75% for a single lens. The discrepancy between the measured and theoretical efficiency results from the imperfect shape of the fabricated triangle pattern. For Au and Ni lenses the efficiency difference from the ideal lens is acceptable. For the diamond lenses it must be considered that due to the weak phase shift of the material very deep structures needed to be fabricated just to achieve necessary effective height with reasonable angles of incidence. This causes more deviations from the optimal structure shape, as can be seen from the SEM images presented in Fig. 2, and also limits the practical use of this type of diamond lenses to lower photon energies (here tested at 5.5 keV).

To demonstrate diffraction-limited focusing down to 100 nm spot size, a set of nickel lenses was characterized at cSAXS and P06 beamlines (SLS and PetraIII, respectively). At cSAXS to illuminate the entire 100 μm × 400 μm entrance aperture coherently enough to obtain diffraction limited focusing a secondary source created by slits close to the source was used. The focal spot was characterized using ptychographic scans over a test object and back-propagating the reconstructed probe signal to the focal plane of the lenses [23–25]. This way a diffraction-limited spot size of 95 nm × 105 nm (FWHM) at 7.2 keV photon energy was measured and confirmed by scanning transmission x-ray microscopy of the same test pattern (Fig. 4). At P06 the same method, including the use of a secondary source, was used to characterize lenses with 400 μm × 440 μm entrance aperture at 8 keV photon energy. The reconstructed diffraction limited spot of 103 nm × 94 nm (FWHM) is presented in Fig. 5. It is worth noting that for this setup the gain in photon flux in the focal spot is about 10^7 when compared to the incident unfocused beam. For an ideal kinoform diffractive Ni lens this would be 1.8×10^7.

#208741 - $15.00 USD Received 24 Mar 2014; revised 12 Jun 2014; accepted 15 Jun 2014; published 30 Jun 2014

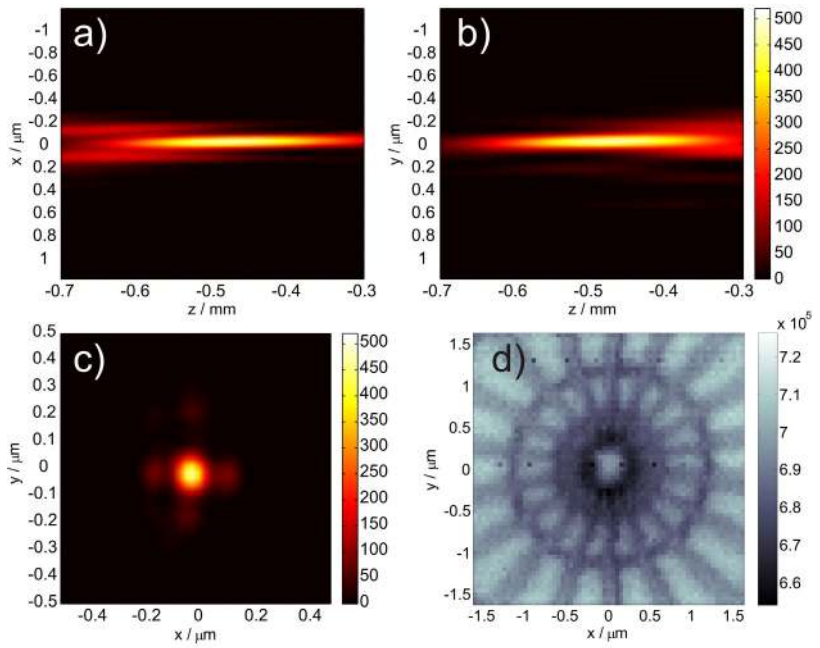

Fig. 4. Ptychographic reconstruction of the probe measured at the cSAXS beamline at SLS. a and b: horizontal (x) and vertical (y) cross sections of the intensity profile of the reconstructed beam. c: profile of the reconstructed beam at the focal plane exhibiting FWHM of 95 nm in x and 105 nm in y direction. d: scanning transmission x-ray microscopy image of a test pattern. Measurement was done at 7.2 keV photon energy using Ni lenses with effective outermost zone width of 100 nm and 100 μm × 400 μm entrance aperture.

For the Ni and Au lenses large part of the losses is due to absorption rather than to unwanted diffraction orders, including the transmitted zeroth order. The ratio of the unwanted diffraction and the focused order can be estimated from the plot in Fig. 3: as the theoretical curve is calculated for the optimal kinoform phase profile, the difference between it and unity is due to absorption. In other words, when the lens is used with the optimal incident angle α, the amount of the unwanted transmitted light equals the difference between the theoretical and measured efficiency value. Looking at the Fig. 3 the difference between the measured efficiency value and that of the ideal profile is 3-5 times smaller than the measured efficiency. This means that in the focal plane 3-5 times as many photons are diffracted into the focal spot compared to all other unwanted orders that are diluted into the background. This has the important consequence that these lenses can be used without central stop and order-sorting aperture (OSA) normally required to filter out the unwanted diffractive orders of Fresnel zone plates. Whereas omitting the OSA increases the background signal and decreases the signal-to-noise ratio (see Fig. 6), it is extremely useful for many applications that require a long working distance, for instance to accommodate bulky sample environment, for optimized placement of fluorescence detectors, or a cryo jet for frozen samples. In practice these benefits often outweigh the increased background level.

#208741 - $15.00 USD Received 24 Mar 2014; revised 12 Jun 2014; accepted 15 Jun 2014; published 30 Jun 2014

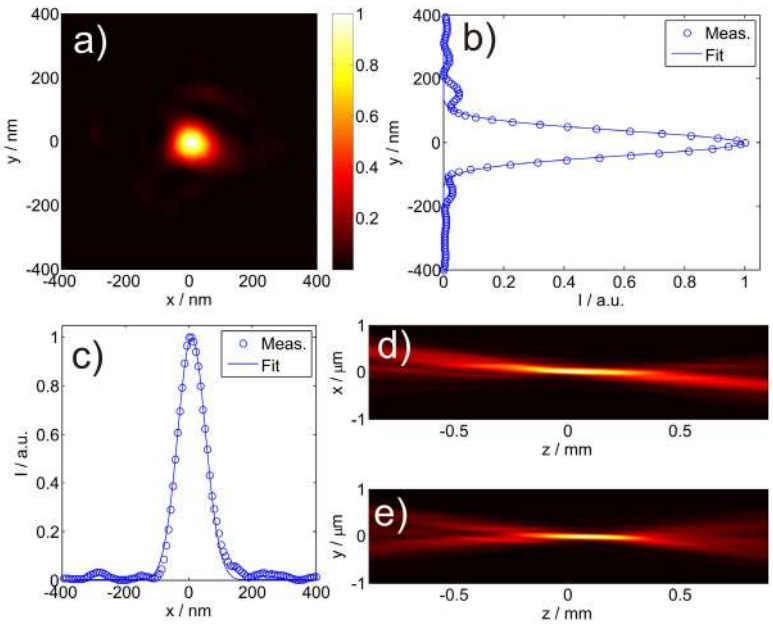

Fig. 5. Ptychographic reconstruction of the probe measured at the beamline P06 at PetraIII. a: cross section of the intensity profile of the reconstructed beam at the focal plane. b and c: vertical (y) and horizontal (x) cross sections, respectively, of the probe in focal plane with gaussian fits exhibiting FWHM of 103 nm in x and 94 nm in y. d and e: horizontal and vertical cross sections of the propagating beam, respectively. Measurement was done at 8 keV photon energy using Ni lenses with effective outermost zone width of 100 nm and 400 µm × 440 µm entrance aperture.

5. Conclusions and outlook

We have designed, fabricated, and experimentally characterized a novel kinoform diffractive x-ray lens. High efficiencies exceeding 50% and diffraction-limited spot sizes down to 100 nm FWHM can be reached. By tuning the incident angle the lenses can be used with a wide band of photon energies: currently we have worked between 5 and 20 keV, but the same concept can be extended even further. The entrance apertures are not limited by the structure height and with current lithographic fabrication techniques the time for lens structure patterning does not constrain the area of the lens. This means that the entrance aperture can be chosen freely to optimize the focusing setup based on the source properties. A good example of this versatility is the nanofocusing module in use at the microXAS beamline: its lenses are mostly used with incoherent illumination over the entrance aperture, thus limiting the spot size to that of the geometrical demagnification of the source size. This means effectively trading off resolution for higher attainable photon flux by using configurations that aim for 200 nm spot size by using lenses with diffraction limit of 100 nm but entrance apertures larger than the transverse coherence length of the source. Using a secondary source created by slits close to the source still remains an option for increased resolution at the cost of photon flux without changing the lenses. This kind of versatility combined with the attainable high efficiency and resolution render this type of lenses a good option for hard x-ray nanofocusing applications at synchrotrons.

#208741 - $15.00 USD Received 24 Mar 2014; revised 12 Jun 2014; accepted 15 Jun 2014; published 30 Jun 2014

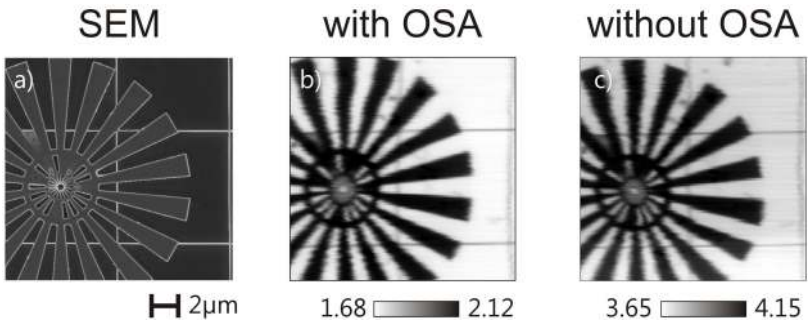

Fig. 6. Evaluation of the effect of the effect of order sorting aperture (OSA). a: SEM image of a gold Siemens star test pattern. b and c: STXM images of the same structure taken at 7.2 keV photon energy using Ni lenses with effective outermost zone width of 100 nm and 100 µm × 400 µm entrance aperture. Units are voltage readings of a photodiode with the same gain setting, so comparable with each other.

We also demonstrated that this type of lens can be made from diamond. The efficiency of these lenses still leaves much more room for improvement compared to their gold and nickel equivalents, and it can be anticipated that progress in the nanostructuring of diamond will result in much higher efficiencies. The low x-ray absorption and excellent thermal stability and heat conductivity of this material will, in combination with the high aperture values make the presented kinoform lenses an excellent choice for use at x-ray free-electron laser (XFEL) sources.

Acknowledgments

The nanofocusing module development and lens characterization were done on the microXAS and cSAXS beamlines at the Swiss Light Source, Paul Scherrer Institut, Switzerland. Additional lens characterization was performed at Hard X-ray Micro/Nano-Probe beamline P06 at PETRA III (DESY) in Hamburg, Germany. This work is supported by the German Ministry of Education and Research (BMBF) under Grant No. 05K10OD1 and by VH-VI-403 of the Impuls- und Vernetzungsfonds (IVF) of the Helmholtz Association of German Research Centres.

#208741 - $15.00 USD Received 24 Mar 2014; revised 12 Jun 2014; accepted 15 Jun 2014; published 30 Jun 2014